Modeling of Wheeled Mobile Robots using Dextrous Manipulation Kinematics

Joseph Auchter, Carl Moore*, Ashitava Ghosal†‡

Abstract—**This document introduces a new kinematic simulation of a wheeled mobile robot operating on uneven terrain. Our modeling method borrows concepts from dextrous manipulation. This allows for an accurate simulation of the way 3-dimensional wheels roll over a smooth ground surface. The purpose of the simulation is to validate a new concept for design of off-road wheel suspensions, called Passive Variable Camber (PVC). We show that PVC eliminates kinematic slip for an outdoor robot. Both forward and inverse kinematics are discussed and simulation results are presented.**

Keywords: kinematics, mobile robots, uneven terrain, dextrous manipulation.

1 Introduction

In recent years, there has been increased interest in robots operating outdoors in unstructured environments [11],[7]. Despite this, the methods used to model mobile robots have not changed much. Traditional wheeled mobile robot (WMR) kinematic modeling (for example, [1]) is inadequate because of the complex nature of the an outdoor robot/ground system. Specifically, assumptions about planar motion and two-dimensional wheels are invalid.

Modeling of WMRs is complex because often there are non-holonomic rolling constraints at the wheel/ground contacts. On uneven terrain the contact point can vary along the surface of the wheel in both lateral and longitudinal directions. Therefore assumptions that the wheel can be modeled as a thin disk and that the linear velocity of the wheel center can be determined by $v = \omega R$ become untenable.

1.1 Kinematic Slip

Accurate modeling of outdoor WMRs is important because unique issues emerge as a result of the unstructured environment. Among them is increased slip between the wheels and the ground. In addition to dynamic slippage due to terrain deformation or insufficient friction, a WMR is affected by kinematic slip [2],[3],[11]. Kinematic slip occurs when there is no instantaneous axis of rotation compatible with all of the robot's wheels. This is the general case on uneven terrain because the wheel/ground contact points vary along the surface of the wheel depending on the terrain shape and robot configuration. Ackermann steering geometry, designed to avoid such slip, works properly only on flat ground.

Wheel slip causes several problems. First, power is wasted [11],[2]. Second, wheel slip reduces the ability of the robot to self-localize because position estimates from wheel encoder data accumulate unbounded error over time [6]. Accurate kinematic models are needed to test robot designs which will potentially reduce this costly kinematic slip.

Sreenivasan and Nanua [10] used screw theory to explore the phenomenon of kinematic slip in wheeled vehicle systems moving on uneven terrain. Modeling two wheels joined by a rigid axle, their analysis showed that kinematic slip can be avoided if the distance between the wheel/ground contact points is allowed to vary. The authors of that work suggest the use of a Variable Length Axle (VLA) with a prismatic joint to achieve the necessary motion. The VLA is difficult to implement because it requires a complex wheel axle design.

As a more practical alternative to the VLA, Chakraborty and Ghosal [2] introduced the idea of adding an extra degree of freedom (DOF) at the wheel/axle joint, allowing the wheel to tilt laterally relative to the axle. This new capability, herein named Passive Variable Camber (PVC), permits the distance between the wheel/ground contact points to change without any prismatic joints. Figure 1 shows an example of an axle and two wheels equipped with PVC.

1.2 Contribution of this work

Traditional methods are not suitable for kinematic modeling of outdoor WMRs due to the complex nature of the terrain/robot system. This document introduces a kinematic simulation of a 3-wheeled mobile robot

*Joseph Auchter (auchtjo@eng.fsu.edu) and Carl Moore (camoore@eng.fsu.edu) are with the Center for Intelligent Systems, Control, and Robotics (CISCOR), FAMU/FSU College of Engineering, Tallahassee, FL, USA.

†Ashitava Ghosal (asitava@mecheng.iisc.ernet.in) is with the Dept. of Mechanical Engineering, Indian Institute of Science, Bangalore, India.

‡The authors would like to thank Patrick Hollis for his insight and assistance with this work.

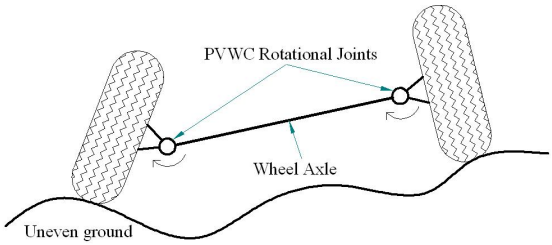

Figure 1: Two tires on uneven ground attached to an axle equipped with Passive Variable Camber. The axis of rotation of each PVC joint is perpendicular to the page.

equipped with PVC and operating on uneven terrain. The work presented here expands upon the simulation of Chakraborty and Ghosal [2], in which the authors made use of kinematic equations of contact originally developed for dextrous manipulation systems. In this is work we extend the analogy by fully formulating the WMR/ground system as a dextrous manipulation problem. This allows for an accurate simulation of the way 3-dimensional wheels roll over a smooth terrain, without many of the assumptions inherent in other modeling techniques. Such fidelity is necessary to study a vehicle with PVC.

The purpose of the simulation is to verify that a WMR equipped with PVC can traverse uneven terrain without kinematic slip. Both forward and inverse kinematics are discussed and simulation results are presented.

2 Analogy Between WMRs and Dextrous Manipulators

In this work a kinematic model of the WMR/ground system is developed using techniques from the field of dextrous manipulation. To our knowledge, the analogy between a robotic hand manipulating an object and a WMR traversing a three-dimensional terrain had never been made before the work of Chakraborty and Ghosal [2]. However, the kinematics of dextrous manipulation provide an ideal description of the way wheels roll over uneven terrain.

A WMR in contact with uneven ground is analogous to a multi-fingered robotic "hand" (the WMR) grasping an "object" (the ground). We hypothesize that the theories relating to manipulator contact and grasping are well-suited to model outdoor vehicles. Table 1 summarizes the analogies between robotic hands and WMRs.

3 Description of Robot

We model a three-wheeled mobile robot (one front and two rear wheels). The front wheel is steerable, and the two rear wheels have PVC joints. The wheels are torus-shaped, which is more realistic than the typical thin-disk model [10].

Table 1: Relationships between manipulators and WMRs

Manipulators	**Mobile Robots**
Multi-fingered hand	Wheeled mobile robot
Grasped object	Ground
Fingers	Wheels
Palm	Robot platform

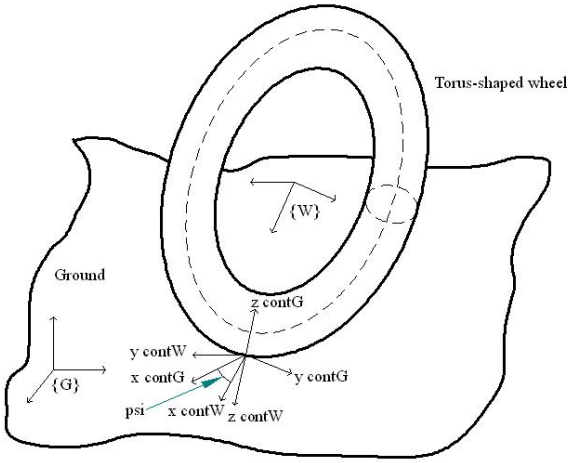

Figure 2: Coordinate frames of the wheel and ground.

Figures 2 and 3 show the coordinate frames which will be used to develop the kinematic equations. Frame $\{G\}$ is the ground reference frame. Frame $\{contG_i\}$ is the ground contact frame for wheel i. The z-axis of $\{contG_i\}$ is the outward normal to the ground surface at the contact point. Frame $\{P\}$ is the robot platform reference frame. $\{A_i\}$ is the frame at the point of attachment of the wheel i to the platform. $\{W_i\}$ is the reference frame of wheel i. $\{contW_i\}$ is the contact frame relative to wheel i. Its z-axis is the outward pointing normal from

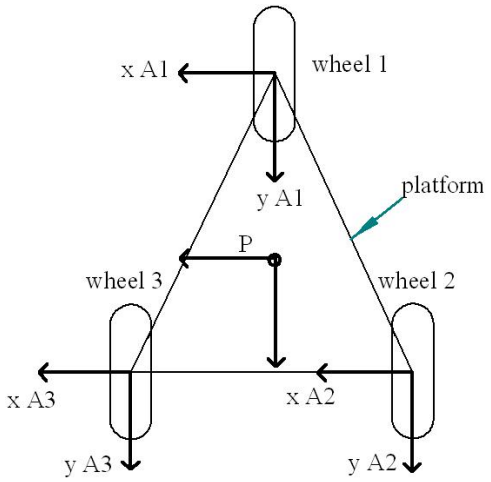

Figure 3: Coordinate frames of the robot platform.

the torus-shaped wheel, which is collinear with the z-axis of $\{contG_i\}$. ψ_i is the angle between the x-axes of frames $\{contG_i\}$ and $\{contW_i\}$.

3.1 Robot Configuration Variables

In this section we introduce the position and velocity variables which describe the state of the robot. We borrow notation from [5] and [9]. The vector of joint velocities is:

$$\dot{\theta} = \left[\dot{\phi}_1 \ \dot{\alpha}_1 \ \dot{\gamma}_2 \ \dot{\alpha}_2 \ \dot{\gamma}_3 \ \dot{\alpha}_3\right]^T$$

where $\dot{\alpha}_i$ is the driving rate of wheel i, $\dot{\phi}_1$ is the steering rate of wheel 1, $\dot{\gamma}_i$ is the rate of tilt of the wheel about the PVC joint of wheel i (for $i = 2, 3$).

The surface S_w of a wheel is parameterized relative to its frame $\{W\}$ by the right-handed orthogonal coordinate chart:

$$f(u, v) : \ U \ \in \ \Re^2 \rightarrow S_w \ \subset \ \Re^3$$

In other words, specifying two parameters u_i and v_i will locate a unique point on the surface of wheel i. This point in the cartesian coordinates of $\{W_i\}$ is $f(u_i, v_i)$. Similarly, the ground surface is parameterized relative to its frame $\{G\}$ by the chart:

$$g(x, y) : \ X \ \in \ \Re^2 \rightarrow S_g \ \subset \ \Re^3$$

meaning that any parameters x and y will locate a unique point $(x, y, g(x, y)) = (x, y, z)$ on the ground surface.

The contact parameters for wheel i are:

$$\eta_i = [u_i \ v_i \ x_i \ y_i \ \psi_i]^T \ , \quad i = 1, 2, 3$$

They are grouped for all three wheels as: $\eta = [\eta_1^T \ \eta_2^T \ \eta_3^T]^T$. Also important are the velocities of the wheel relative to the ground:

$$^{contW}V_{GW} = V_c = [v_x \ v_y \ v_z \ \omega_x \ \omega_y \ \omega_z]^T \qquad (1)$$

The leading superscript indicates that the vector is resolved in the $\{contW\}$ frame.

4 Robot Kinematics

In this section we formulate the forward and inverse kinematics for the robot. First, some tools will be developed (following [5]) which will contribute to the formulation.

The robot/ground system is modeled as a hybrid series-parallel mechanism. Each wheel is itself a kinematic chain between the platform and the ground, and there are three such chains in parallel. The *closure constraint* [9] for the parallel mechanism specifies that each kinematic chain must end at the same frame (in this case, $\{G\}$). Let T_{AB} be the 4×4 homogeneous rigid body transform between frames A and B. Then the closure constraint for the robot is:

$$T_{PG,wheel1} = T_{PG,wheel2} = T_{PG,wheel3} \qquad (2)$$

The way the wheel/ground contact is modeled determines what types of relative motion are allowed between the two surfaces. We model the wheel/ground interaction as a point contact with friction. This means that $\{contW\}$ and $\{contG\}$) frames do not translate relative to each other. Relative rolling is permitted. Mathematically, this is expressed as:

$$V_c = \bar{B} \ \tilde{V}_c \qquad (3)$$

where

$$\bar{B} = \begin{bmatrix} 0_{3\times3} \\ I_{3\times3} \end{bmatrix}$$

for each wheel/ground contact. $\tilde{V}_c$, a subset of V_c (equation (1)), are called the allowable contact velocities. For point contact with friction $\tilde{V}_c = [\omega_x \ \omega_y \ \omega_z]^T$.

Montana [8] developed kinematic equations which describe how two arbitrarily-shaped, smooth surfaces roll/slide against each other. In our case, the two surfaces are the wheel and ground. Metric (M), curvature (K), and torsion (T) forms are used to describe the ground and wheel surfaces. The equations for rolling contact are:

$$\begin{aligned} (\dot{u}, \dot{v})^T &= M_w^{-1} \left(K_w + K^*\right)^{-1} (-\omega_y, \omega_x)^T \\ (\dot{x}, \dot{y})^T &= M_g^{-1} R_\psi \left(K_w + K^*\right)^{-1} (-\omega_y, \omega_x)^T \\ \dot{\psi} &= \omega_z + T_w M_w \left(\dot{u}, \dot{v}\right)^T + T_g M_g \left(\dot{x}, \dot{y}\right)^T \end{aligned} \qquad (4)$$

The inputs to these equations are the allowable contact velocities $\tilde{V}_c$, and the outputs are $\dot{\eta}$.

Ad_{AB} is the 6×6 adjoint transform [9] which changes the frame of reference of a 6×1 velocity vector from $\{B\}$ to $\{A\}$. Let $Q_i = Ad_{W_i \, contW_i} \ \bar{B}$. The ground and contact Jacobian is defined as:

$$J_{GC} = \begin{bmatrix} Ad_{W_1G} & Q_1 & & 0 \\ Ad_{W_2G} & & Q_2 & \\ Ad_{W_3G} & 0 & & Q_3 \end{bmatrix} \qquad (5)$$

Let the Jacobian for wheel 1 (front wheel) be defined as:

$$^P J_{PW_1} = \begin{bmatrix} \left(\frac{\partial T_{PW_1}}{\partial \phi_1} \ T_{PW_1}^{-1}\right)^\vee , & \left(\frac{\partial T_{PW_1}}{\partial \alpha_1} \ T_{PW_1}^{-1}\right)^\vee \end{bmatrix}$$

where the leading superscript indicates that this Jacobian is in the so-called "spatial" form, meaning relative to frame $\{P\}$. The `vee` operator $\vee$ extracts the vector components from the 4x4 skew-symmetric representation:

$$\begin{bmatrix} 0 & -\omega_z & \omega_y & v_x \\ \omega_z & 0 & -\omega_x & v_y \\ -\omega_y & \omega_x & 0 & v_z \\ 0 & 0 & 0 & 1 \end{bmatrix}^\vee = \begin{bmatrix} v_x \\ v_y \\ v_z \\ \omega_x \\ \omega_y \\ \omega_z \end{bmatrix}$$

The Jacobians for wheels 2 and 3 are similar, except that ϕ is replaced with γ and the subscripts are changed appropriately. Transformed into the wheel frame:

$$J_{W_1} = Ad_{W_1P} \cdot \ ^P J_{PW_1}$$

Similarly for wheels 2 and 3. The total robot Jacobian is then:

$$J_R = \begin{bmatrix} J_{W_1} & & 0 \\ & J_{W_2} & \\ 0 & & J_{W_3} \end{bmatrix} \quad (6)$$

Let $\tilde{V}_{GC} = \begin{bmatrix} {}^G V_{PG}^T & \tilde{V}_{C_1}^T & \tilde{V}_{C_2}^T & \tilde{V}_{C_3}^T \end{bmatrix}^T \in \Re^{15}$. This vector is known as the ground and contact velocities. ${}^G V_{PG}$ is the 6×1 vector of velocities of the *ground relative to the platform*, resolved in the ground reference frame. The motion of the platform relative to the ground is simply: ${}^G V_{GP} = -{}^G V_{PG}$.

The constraint equation relating the joint velocities to the ground and contact velocities is [5]:

$$J_{GC}\ \tilde{V}_{GC} = J_R\ \dot{\theta} \quad (7)$$

Note that in the general case, neither J_{GC} nor J_R are square, and thus are not invertible. For the forward and inverse kinematics we have adopted the methods of [4] and [5], originally developed for dextrous manipulators.

4.1 Forward Kinematics

In this section, our algorithm for the forward kinematic simulation of the three-wheeled mobile robot is introduced. Table 2 shows the desired inputs and outputs for the forward kinematics.

Table 2: Forward kinematics inputs and outputs

Inputs	Outputs
Desired wheel joint velocities $\dot{\theta}$	Platform and contact velocities $\tilde{V}_{GC}$

Let c be the number of columns of J_{GC}. The singular value decomposition of matrix J_{GC} is:

$$J_{GC} = U\ \Sigma\ V^T$$

Let $r = rank(J_{GC})$. Split U into $[U_1\ U_2]$, where $U_2 \in \Re^{c \times (c-r)}$. Then the constraints (7) can be re-written as:

$$U_2^T\ J_R\ \dot{\theta} = 0 \quad (8)$$

If a chosen set of inputs $\dot{\theta}$ satisfies (8) then a necessary and sufficient condition to uniquely determine a set of outputs $\tilde{V}_{GC}$ is: $rank(J_{GC}) = length(\tilde{V}_{GC})$. Then $\tilde{V}_{GC}$ can be found using the generalized (pseudo) inverse of J_{GC}:

$$\tilde{V}_{GC} = (J_{GC})^+\ J_R\ \dot{\theta} = (J_{GC}^T\ J_{GC})^{-1}\ J_{GC}^T\ J_R\ \dot{\theta} \quad (9)$$

See [5] for more details about these derivations.

Algorithm for the forward kinematic simulation

1. *Choose guess values for initial conditions (θ_0 and η_0). Use Matlab's* `fsolve` *routine to optimize the initial conditions such that they obey the closure constraints (2).*
2. *Calculate J_{GC} and J_R according to (5) and (6), respectively.*
3. *Choose a set of desired inputs $\dot{\theta}_d$. If first time step, choose any desired $\dot{\theta}_d$. Otherwise, choose $\dot{\theta}$ from the previous time step. Use* `fsolve` *to adjust them to obey the constraints (8).*
4. *Check to make sure that J_{GC} is full column rank. If not, exit simulation.*
5. *Calculate outputs $\tilde{V}_{GC}$ according to (9).*
6. *Calculate the velocities of the contact variables, using the equations (4): $\dot{\eta} = F(\tilde{V}_{GC})$.*
7. *Integrate the velocities $\dot{\eta}$ and $\dot{\theta}$ to get the positions for the next time step.*
8. *Return to step 2 with the new values of θ and η. Continue to loop until end of simulation.*

Note that the equations (8) depend on the configuration of the robot, which changes with time. These constraints prevent us from arbitrarily choosing the inputs $\dot{\theta}$, necessitating the optimization of step 3.

Forward Kinematics Results: The forward kinematics simulation was run on several different surfaces and for different inputs. Here we present results for a 5-second simulation on a randomly-generated terrain with the following desired inputs: $\dot{\theta}_d = [0\ 1\ 0\ 1\ 0\ 1]^T$. Figure 4 shows the robot in contact with the surface at the end of the simulation. Figure 5 plots the $\dot{\theta}$ inputs and the steering and PVC angles. Figure 6 plots the paths of the 3 wheel/ground contact points in the ground x-y plane. It also shows the projections of the wheel centers in that plane, to show that the wheels tilt as the robot traverses the uneven terrain.

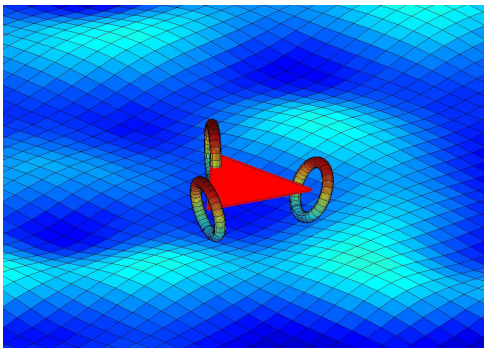

Figure 4: The wheeled mobile robot on the ground surface.

Figure 5 shows that the inputs start at the desired values and then follow smooth trajectories through the input space such that the constraints (8) are satisfied. Figure 7

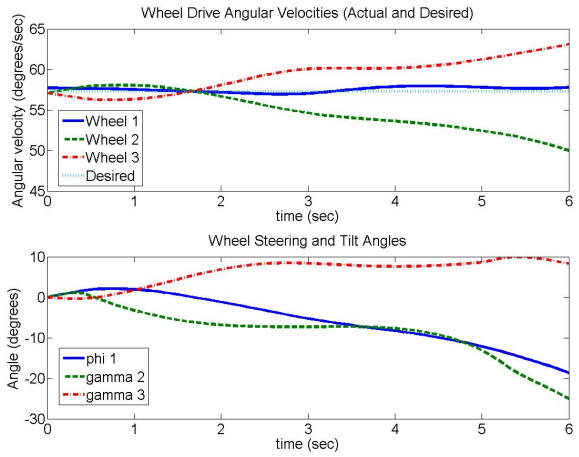

Figure 5: The forward kinematic inputs: wheel drive rates, steering angle, and tilting angles.

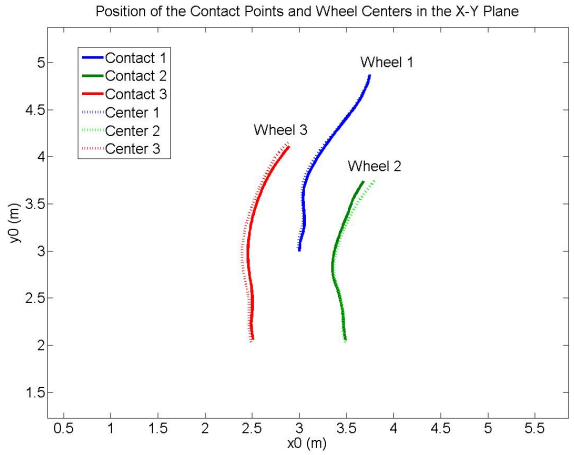

Figure 6: The wheel/ground contact points and wheel centers in the xG-yG plane.

plots the errors in satisfaction of the constraints (7) and the rolling contact kinematic equations (4), as defined by:

$$\begin{aligned} r_1 &= J_{GC}\,\tilde{V}_{GC} - J_R\,\dot{\theta} \\ error_1 &= (r_1^T\, r_1)^{1/2} \\ r_2 &= \dot{\eta} - F(\tilde{V}_{GC}) \\ error_2 &= (r_2^T\, r_2)^{1/2} \end{aligned} \tag{10}$$

Figure 7 shows that the constraint equations are well satisfied during the course of the simulation.

4.2 Inverse Kinematics

In this section, our inverse kinematic simulation is introduced. The development is very similar to that for the forward kinematics. Table 3 the desired inputs and outputs for the inverse kinematics.

In principle, any or all of the ground and contact velocities $\tilde{V}_{GC}$ could be chosen and then adjusted via an optimization routine to obey the constraints (7). However in practice only the x and y velocities of the platform center of gravity (CG) (the first two elements of the vector $\tilde{V}_{GC}$) might be of interest to a motion planner.

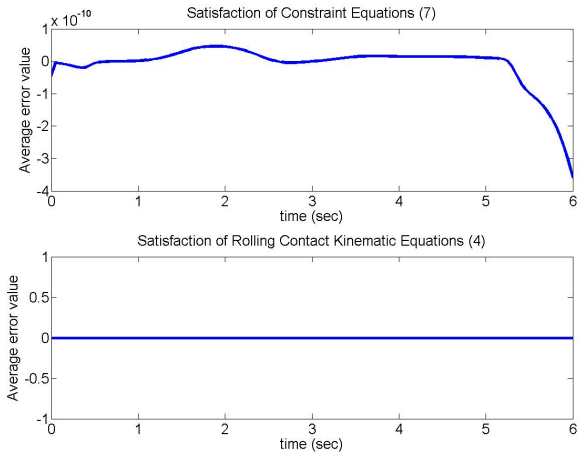

Figure 7: Errors in satisfaction of constraint equations (7) and (4).

Table 3: Inverse kinematics inputs and outputs

Inputs	Outputs
Platform and contact velocities $\tilde{V}_{GC}$	Desired wheel joint velocities $\dot{\theta}$

Let c be the number of columns of J_R. The singular value decomposition of matrix J_R is:

$$J_R = U\ \Sigma\ V$$

Let $r = rank(J_R)$. Split U into $[U_1\ U_2]$, where $U_2 \in \Re^{c\times(c-r)}$. Then the constraints (7) can be re-written as:

$$U_2^T\ J_{GC}\ \tilde{V}_{GC} = 0 \tag{11}$$

If a chosen set of inputs $\tilde{V}_{GC}$ satisfies (11) then a necessary and sufficient condition to uniquely determine a set of outputs $\dot{\theta}$ is: $rank(J_R) = length(\dot{\theta})$. Then $\dot{\theta}$ can be found using the generalized (pseudo) inverse of J_R:

$$\dot{\theta} = (J_R)^+\ J_{GC}\ \tilde{V}_{GC} = (J_R^T\ J_R)^{-1}\ J_R^T\ J_{GC}\ \tilde{V}_{GC} \tag{12}$$

See [4] for more details about these derivations. The algorithm for the inverse kinematics is similar to that of the forward case.

Inverse Kinematics Results: The inverse kinematics were tested on several types of terrain. Here we present results for a randomly-generated uneven surface. The desired input velocities for the platform CG were: $\dot{x}_{CG} = 0$, $\dot{y}_{CG} = 0.5$. The linear and angular velocities of the platform CG frame relative to the ground are plotted in figure 8. Figure 9 plots the outputs of the inverse kinematics: the wheel joint velocities $\dot{\theta}$.

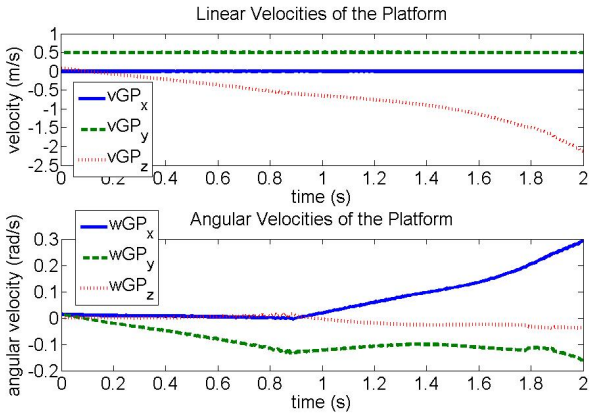

Figure 8: The robot platform velocities relative to the ground.

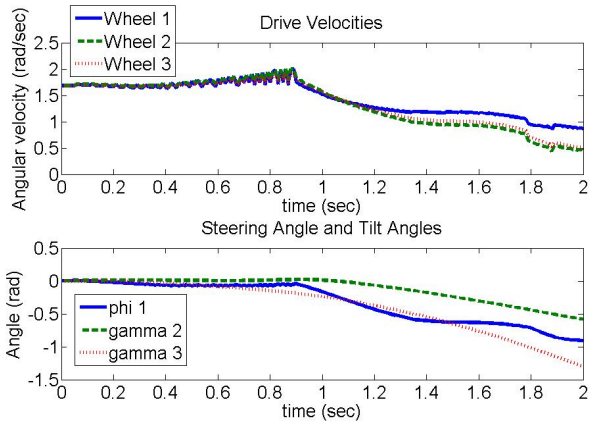

Figure 9: The wheel joint velocities: steering, driving, and tilting.

5 Conclusion and Future Work

We have introduced a new method for simulating wheeled mobile robots moving on arbitrary uneven terrains such as those found outdoors. Our method models the robot/ground system using concepts developed for dextrous manipulators. This allows for precise modeling of the way wheels roll over uneven terrain. The purpose of the simulation is to validate a new concept for design of off-road vehicle wheel suspensions. The kinematic simulation described in this document shows that Passive Variable Camber eliminates kinematic slip when applied to an outdoor robot.

We are currently working on making the simulation more robust and accurate for longer simulations. Position error accumulates due to inaccuracies in the velocity integration (step 7 of the algorithm), so we are investigating ways to enforce the holonomic position constraints.

Next, results from the field of motion planning for dextrous manipulators will be applied to the wheeled mobile robot motion planning and navigation problem. Our simulation will be used to verify that the robot can navigate from an initial to a final configuration without wheel slip. PVC's effects on power consumption and localization ability will be explored in future versions of the simulation.

References

[1] Alexander, J.C., Maddocks, J.H. 1989. "On the Kinematics of Wheeled Mobile Robots". *The Intl. J. of Robotics Research*, Vol. 8, No. 5, 15-27.

[2] Chakraborty, N., Ghosal, A. 2004. "Kinematics of Wheeled Mobile Robots on Uneven Terrain". *Mech. and Machine Theory*. Vol. 39, no. 12, pp. 1273-1287.

[3] Choi, B., Sreenivasan, S., Davis, P. 1999. "Two Wheels Connected by an Unactuated Variable Length Axle on Uneven Ground: Kinematic Modeling and Experiments". *ASME Journal of Mech Des.* Vol. 121, pp. 235-240.

[4] Han, L., Trinkle, J.C. 1998. "The Instantaneous Kinematics of Manipulation". *Proc. 1998 IEEE ICRA*, pg. 1944-1949.

[5] Han, L., Trinkle, J.C., and Li, Z.X. 1997. "The Instantaneous Kinematics and Planning of Dextrous Manipulation". *Proc. 1997 IEEE Intl. Symp. on Assembly and Task Planning*, pg. 60-65.

[6] Huntsberger, et al. 2002. "Rover Autonomy for Long Range Navigation and Science Data Acquisition on Planetary Surfaces". *Proc. of 2002 IEEE ICRA*.

[7] Iagnemma, K., et al. 2003. "Experimental Study of High-speed Rough-terrain Mobile Robot Models for Reactive Behaviors". *Springer Tracts in Advanced Robotics*. Vol. 5, pp. 654-663.

[8] Montana, D. 1988. "The Kinematics of Contact and Grasp". *The International Journal of Robotics Research*, Vol. 7, No. 3, 17-32.

[9] Murray, R., Li, Z., and Sastry, S. 1994. *A Mathematical Introduction to Robotic Manipulation*. CRC Press: Boca Raton.

[10] Sreenivasan, S.V., Nanua, P. 1999. "Kinematic Geometry of Wheeled Vehicle Systems". *Trans. of the ASME J. of Mech. Des.*, Vol. 121.

[11] Waldron, K. 1994. "Terrain Adaptive Vehicles". *ASME Journal of Mech Des.* Vol 117, pp. 107-112.